

Assessment of exhaust emissions from carbon nanotube production and particle collection by sampling filters

Candace Su-Jung Tsai, Mario Hofmann, Marilyn Hallock, Michael Ellenbecker & Jing Kong

To cite this article: Candace Su-Jung Tsai, Mario Hofmann, Marilyn Hallock, Michael Ellenbecker & Jing Kong (2015) Assessment of exhaust emissions from carbon nanotube production and particle collection by sampling filters, Journal of the Air & Waste Management Association, 65:11, 1376-1385, DOI: [10.1080/10962247.2015.1095812](https://doi.org/10.1080/10962247.2015.1095812)

To link to this article: <http://dx.doi.org/10.1080/10962247.2015.1095812>

 View supplementary material 

 Published online: 20 Oct 2015.

 Submit your article to this journal 

 Article views: 146

 View related articles 

 View Crossmark data 

Assessment of exhaust emissions from carbon nanotube production and particle collection by sampling filters

Candace Su-Jung Tsai,^{1,2,*} Mario Hofmann,³ Marilyn Hallock,⁴ Michael Ellenbecker,⁵ and Jing Kong⁶

¹Department of Environmental and Radiological Health Science, College of Veterinary Medicine and Biomedical Science, Colorado State University, Fort Collins, CO, USA

²Birck Nanotechnology Center, Discovery Park, Purdue University, West Lafayette, IN, USA

³Department of Materials Science and Engineering, National Cheng Kung University, Tainan, Taiwan, Republic of China

⁴Department of Environment, Health and Safety, Massachusetts Institute of Technology, Cambridge, MA, USA

⁵Toxics Use Reduction Institute, University of Massachusetts Lowell, Lowell, MA, USA

⁶Department of Electrical Engineering and Computer Science, Massachusetts Institute of Technology, Cambridge, MA, USA

*Please address correspondence to Candace Su-Jung Tsai, Department of Environmental and Radiological Health Science, College of Veterinary Medicine and Biomedical Science, Colorado State University, 1681 Campus Delivery, EH Room 153, Fort Collins, Colorado 80523-168, USA; e-mail: Candace.Tsai@colostate.edu

This study performed a workplace evaluation of emission control using available air sampling filters and characterized the emitted particles captured in filters. Characterized particles were contained in the exhaust gas released from carbon nanotube (CNT) synthesis using chemical vapor deposition (CVD). Emitted nanoparticles were collected on grids to be analyzed using transmission electron microscopy (TEM). CNT clusters in the exhaust gas were collected on filters for investigation. Three types of filters, including Nalgene surfactant-free cellulose acetate (SFCA), Pall A/E glass fiber, and Whatman QMA quartz filters, were evaluated as emission control measures, and particles deposited in the filters were characterized using scanning transmission electron microscopy (STEM) to further understand the nature of particles emitted from this CNT production. STEM analysis for collected particles on filters found that particles deposited on filter fibers had a similar morphology on all three filters, that is, hydrophobic agglomerates forming circular beaded clusters on hydrophilic filter fibers on the collecting side of the filter. CNT agglomerates were found trapped underneath the filter surface. The particle agglomerates consisted mostly of elemental carbon regardless of the shapes. Most particles were trapped in filters and no particles were found in the exhaust downstream from A/E and quartz filters, while a few nanometer-sized and submicrometer-sized individual particles and filament agglomerates were found downstream from the SFCA filter. The number concentration of particles with diameters from 5 nm to 20 μm was measured while collecting particles on grids at the exhaust piping. Total number concentration was reduced from an average of 88,500 to 700 $\text{particle}/\text{cm}^3$ for the lowest found for all filters used. Overall, the quartz filter showed the most consistent and highest particle reduction control, and exhaust particles containing nanotubes were successfully collected and trapped inside this filter.

Implications: As concern for the toxicity of engineered nanoparticles grows, there is a need to characterize emission from carbon nanotube synthesis processes and to investigate methods to prevent their environmental release. At this time, the particles emitted from synthesis were not well characterized when collected on filters, and limited information was available about filter performance to such emission. This field study used readily available sampling filters to collect nanoparticles from the exhaust gas of a carbon nanotube furnace. New agglomerates were found on filters from such emitted particles, and the performance of using the filters studied was encouraging in terms of capturing emissions from carbon nanotube synthesis.

Introduction

A “nanoparticle” as referred in this paper is a particle with at least one dimension less than 100 nm (Maynard and Kuempel, 2005); this definition applies to carbon nanotubes (CNTs), which are less than 100 nm in diameter with lengths that can be orders of magnitude longer than 100 nm. Emissions from manufacturing nanomaterials using processes such as chemical

vapor deposition (CVD) are of concern since they may lead to human and environmental exposure. In a previous publication (Tsai et al., 2009), CNT filaments and carbon nanoparticles in clusters were found among the particles in the exhaust from a CVD furnace. Monodispersed CNTs generated in the laboratory with a controlled size have been evaluated for filtration collection efficiency using a “medium performance glass fiber

filter,” and fibrous CNTs longer than 300 nm were collected with increased efficiency compared to spherical particles (Seto et al., 2010). However, methods to control air emissions from workplace carbon nanotube production have not been evaluated in the published literature. Such emissions would contain a mixture of aerosol by-products generated during synthesis that will be different from the well-controlled CNTs products being used in most studies. It is important to mitigate the environmental and occupational health effects caused by nanoparticles in general and CNTs in particular due to the potential adverse effects to humans (Shvedova et al., 2005; Shvedova et al., 2008; Ma-Hock et al., 2009; Shvedova et al., 2008; Ma-Hock et al., 2009). Of particular concern are studies that found asbestos-like carcinogenic effects in mice (Ryman-Rasmussen et al., 2009; Takagi et al., 2008; Poland et al., 2008; Takagi et al., 2008; Poland et al., 2008) from multiwalled CNT (MWCNT) exposure. Recently, the International Agency for Research on Cancer (IARC) classified MWCNT type 7 as a 2B suspect human carcinogen (Grosse et al., 2014). Since at least some CNTs are likely to be carcinogenic, CNT emissions during production processes must be better understood to the forms of emitted particles and be controlled in order to prevent and manage their release into the atmosphere.

Because asbestos-like carcinogenic effects have been found associated with CNT exposure (Ryman-Rasmussen et al., 2009; Takagi et al., 2008; Poland et al., 2008) there is a significant cancer risk, and the Occupational Safety and Health Administration (OSHA) 8-hr time-weighted average permissible exposure limit for worker exposure to asbestos is only 0.1 fibers/cm³ (OSHA, 2006); if CNT exposures are to be kept to levels anywhere near that required for asbestos, effective controls must be utilized. An area of active research is the ability of currently available filters to capture nanoparticles to manage the release.

In this project, aerosols emitted from a CVD furnace containing nanometer- and micrometer-sized particles were analysed, and the use of sampling filters to collect emitted particles as a control measure was examined to evaluate this control performance and characterize emitted carbon nanotubes. Some published studies have shown that some commercially available pollution control tools and respiratory protection filters were sufficient for collecting nanoparticles (Rengasamy, Eimer, and Shaffer, 2009; Tsai et al., 2012; Tsai et al., 2012). Particularly, some studies showed the CNT deposition on common aerosol filters for collecting aerosolized CNT products and found CNTs were collected through an interception mechanism (Seto et al., 2010; Wang and Pui, 2013; Wang and Otani, 2012). The high-efficiency particulate air (HEPA) filters have been found to provide close to 100% collection efficiency in the nanoparticle size range (Rengasamy et al., 2008; Golanski et al., 2009; Golanski, Guiot, and Tardif, 2008; Golanski, Guiot, and Tardif, 2010). However, for the purpose of characterizing captured particles, practical limitations in the use of a HEPA filter for this process are such that collected particles could not be further characterized using scanning electron microscopy (SEM). Air sampling filters were appropriate for collecting CNT furnace exhausts in this study.

A previous study by the authors investigated particle concentration, morphology, and composition of aerosols in the exhaust

from a CVD furnace, and found that significant emission of carbon fibers, nanotubes, and iron oxide nanoparticles to the environment was of concern (Tsai et al., 2009). A study by Tsai et al. has investigated filtration efficiency while collecting silica nanoparticles and found a range of collection efficiencies for eight filters, including environmental fabric filters and particle sampling filters, that is, quartz and fiberglass filters (Tsai et al., 2012). A study by Ji et al. (2015) reported that the use of a fabric filter system provided only 20% particle collection for TiO₂ at a particle diameter of 100 nm. Deposition of CNTs on glass fiber, mixed cellulose ester, polycarbonate, and polyvinyl chloride filters was studied by Smith and Bach (2015) using aerosolized commercial CNTs products, and they concluded that methods to enable the visualization of the number of particles and their shapes, sizes, and states of agglomeration for deposited CNTs are important and need to be accomplished. This current study addresses the important and required analysis of those missing elements just described. Since most furnace operations for CNT production utilize high temperature, a 1975 study investigating the loading characteristics of quartz fiber filters for nonvolatile particles at high temperatures is relevant if the high-temperature emissions will be collected (Lundgren and Gunderson, 1975). Lundgren and Gunderson found increasing collection efficiency for submicrometer particles with increasing temperature, and they stated that the main problems encountered at elevated temperatures were vaporization of volatile particles and mechanical leakage of the filter holder (Lundgren and Gunderson, 1975). Glass-fiber filters were studied also in comparison to quartz by Lundgren and Gunderson for environmental application in 1976 (Lundgren and Gunderson, 1976). Both glass-fiber and microquartz fiber filters were evaluated over temperatures ranging from 20°C to 540°C (68°F to 1004°F), particle diameters from 0.05 to 26 μm, and a range of gas velocities and particle volatilities. They concluded for both filters that nonvolatile particle penetration decreased with increasing temperature and increasing filter loading, and the effect of elevated temperature on particle collection characteristics was not a determining factor in application of high-efficiency filters. That indicates a sustainable practical use for managing emission of furnace operation.

The practical application of filters for CNT furnaces emitting nanotubes and carbon fibers has yet to be studied. There is still a lack of information about the characteristics of the particles emitted and collected from CNT production. In this study, nanoparticles emitted from a CVD furnace were characterized using real-time instrumentation techniques and electron microscopy, while nanometer- and micrometer-sized particles were collected on filters. Three types of filters were chosen to study, including two air sampling filters, that is, quartz and fiberglass (A/E) filters, since previous results found greater than 92% collection efficiency of nanoparticles at 2.3 m/min filtration velocity (Tsai et al., 2012). One filter commonly used in laboratories for water filtration was chosen for comparison. This filter was being used to filter the furnace exhaust at the facility evaluated here. The practical use of these filters was investigated particularly for collecting CNT, filaments, and carbon nanoparticles, and the release of such particles was studied. This study aimed to evaluate (1) the

characteristics of particles collected from the exhaust gas and (2) the filter performance under typical use conditions.

Materials and Methods

Synthesis process

All experiments were performed in a common laboratory CVD setup consisting of a fused silica cylindrical reactor chamber 2.5 cm in diameter and 60 cm in length heated by a clamshell furnace located in a laboratory constant velocity fume hood (Kewaunee). Aerosol-assisted CVD was used to generate MWCNTs at high yield (Xiang et al., 2007). In this approach, both the catalyst and the carbon feedstock were continuously introduced into the reaction zone during the 20-min CVD process by evaporating a solution of ferrocene and cyclohexane at a feeding rate of 10 mL/hr from a heated nozzle. The reaction temperature typically was 800°C and a gas stream of 500 sccm³/min Ar and 50 sccm³/min H₂ was used. The continuous introduction of catalyst and carbon feedstock in the growth of MWCNTs creates high-density films deposited on substrates and used for structural applications. The study was performed at two temperature conditions, which formed differing numbers of fibrous or spherical particles. The furnace was first operated at the normal temperature of 800°C, which produced more CNTs and fibrous by-products in the exhaust. After the three filters were tested, the furnace was operated at a higher temperature (925°C), which produced more spherical carbon particles and small fiber filaments.

Particle measurement

Two instruments were operated simultaneously to record airborne particle concentrations in the exhaust stream during MWCNT production; particle concentration and size distribution were recorded every second. The concentrations of airborne individual and agglomerate nanoparticles for diameters from 5.6 to 560 nm were measured using the Fast Mobility Particle Sizer (FMPS) spectrometer (TSI, model 3091, Shoreview, MN) operated at an airflow of 10 L/min, with 32 channels of resolution (16 channels per decade). The FMPS performs particle size classification based on differential electrical mobility classification. The concentrations of airborne particles for diameters from 0.5 to 20 μm were measured using the Aerodynamic Particle Sizer (APS) spectrometer (TSI, model 3321, Shoreview, MN) operated at an airflow of 5 L/min in parallel with the measurements taken by FMPS. The APS provides high-resolution, real-time aerodynamic measurements of particle size. Normalized particle number concentrations measured by the FMPS and APS were calculated in each size channel based on the average concentration during each measurement time period. Carbon-impregnated conductive silicon tubing (2 m) was connected to the air inlet of FMPS and APS to reach the measurement locations. The total particle loss in the 2-m conductive tubing was found to be ≤5% for particle diameters >10 nm (Tsai, 2015). The measured particle

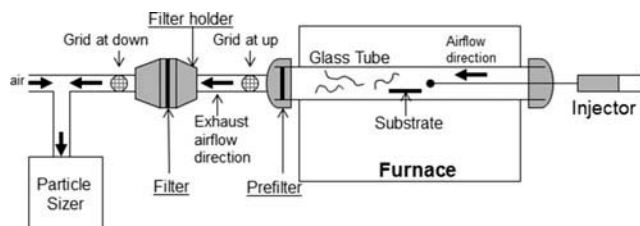


Figure 1. Illustration of experimental setup. Placements of TEM grids are shown as small grid circles, which were upstream (grid at up) and downstream (grid at down) of the filter. Exhaust airflow is 2 L/min; the airflow to particle sizer is 10 (FMPS) L/min or 5 (APS) L/min.

concentration was not adjusted for the line loss, due to the comparison of relative data in this study so the losses could be ignored.

Particle concentrations in the exhaust gas were measured in the gas stream after passing through the filter under test and compared to the gas stream without using a filter to determine the reduction in particle concentration and the change in particle size distribution. The experimental setup is shown in Figure 1. The measurements by FMPS (10 L/min) and APS (5 L/min) were taken individually and the exhaust (2 L/min) particle concentrations were calculated considering the ratio of compensating room air flow to furnace exhaust flow after subtracting the room air concentration, termed the adjusted concentration.

Nanoparticle sampling method

Aerosol nanoparticles were collected on grids for transmission electron microscopic (TEM) analysis to provide information about particle morphology and elemental composition. This sampling method was targeted to capture nanosized particles through Brownian motion when airstreams pass through the grid-coated film surface. TEM grids (SPI 400 mesh copper grid with a Formvar/carbon film) were placed in line with the exhaust air tube (3 mm ID); airstream flow direction is shown in Figure 1. The tubing's internal diameter is the same as the grid's diameter, the grid was inserted vertically in the tubing, and air flowed through on both sides of grid surface. The upstream location (grid at up, noted in Figure 1) was directly connected at the exhaust outlet, and the downstream location (grid at down, noted in Figure 1) was connected at the exhaust of the filter. When the filter was not used, the grid was placed only at the upstream location. Particle samples were taken simultaneously with concentration measurements for each synthesis operation. The sampled particles on the grid were analyzed to characterize emitted nanoparticles in the exhaust gas and in the gas downstream from the filter.

Particle collection on filters

Three types of filters, including Nalgene surfactant-free cellulose acetate (SFCA; 75 mm D, 0.2–0.45 μm pore size, VWR, Radnor, PA), Pall A/E glass fiber (47 mm D, Mesa Labs, Butler, NJ; called A/E), and Whatman QMA quartz fiber (47 mm D, Mesa Labs, Butler, NJ; called quartz) filters

were used. The A/E and quartz filters were selected as being representative of standard high-efficiency air filters widely available on the market; these filters are designed and marketed for aerosol sampling and filtration of small exhaust gas streams, such as the CNT furnace exhaust in this study, and are similar to the glass and quartz filters studied by Lundgren and Gunderson (1975, 1976). The SFCA filter was tested for a comparison to high-efficiency aerosol filters. Users of small CVD furnaces such as the one evaluated here may be tempted to employ filters such as the SFCA filter on the furnace exhaust gas stream since they are commonly available in laboratories; this was in fact the practice at the evaluated laboratory. A better option would be, of course, to use a HEPA filter, but the laboratory would have to purchase such a filter in a housing of a proper size and integrate that housing into the furnace exhaust system. The effort entailed in this may lead the laboratory to use a simpler filter that is already available in the laboratory.

The A/E filter is described by its manufacturer as a binder-free borosilicate glass-fiber filter that, according to the online product description, is “recommended by EPA for high-volume air sampling to collect atmospheric particles and aerosols.” According to the manufacturer, the quartz filter is designed for air sampling in high temperature, for high-acid environments, and for PM-10 testing. The A/E and quartz filters have claimed collection efficiencies of >99.98% and >99.95%, respectively, for a particle diameter of 0.3 μm (Pall Corporation, 2011; Whatman GE Healthcare, 2011)

A stainless-steel filter holder (F1 closed face filter holder, 47 mm D, Mesa Labs, Butler, NJ) was installed at the exhaust outlet approximately 15 cm from the flange of the reactor glass tube. A single SFCA filter was used as a prefilter and inserted at the exit of the synthesis glass tube in addition to using the individual test filter. This double filter application was used to prefilter out some large carbon particles being fed to the test filters, and had no effect on the performance of measured test filters. Filter performance was studied by characterizing deposited particles, characterizing filter porosity, and comparing particle concentrations measured in the exhaust gas.

Analysis of aerosol particles on filter

Sampled aerosol particles from the exhaust gas were characterized using scanning transmission electron microscopy (STEM), TEM, and energy-dispersive spectroscopy (EDS). Particles collected on grids were analyzed using TEM and particles on filters were analyzed using STEM. STEM images of the filter samples were collected using a field emission scanning electron microscope (JSM-7401F, JEOL, Peabody, MA) operated at accelerating voltages of 0.8–15 kV, and an FEI Nova DualBeam SEM/FIB instrument, operated at 10 kV and 2.1 nA, was used to collect SEM images and XEDS data. (The XEDS detector was an Oxford XMAX and the analysis software is Oxford Aztec.) The STEM by JSM-7401F images were obtained using a transmitted electron detector attachment to the scanning electron microscope and with the microscope operated at an accelerating voltage of 20 kV. Elemental analysis was performed using an EDS attachment of the STEM (EDAX) with primary electron beam excitation energy

of 10 kV. TEM images of the samples were taken using either a Philips EM400 TEM (Philips, Eindhoven, The Netherlands) operated at 100kV or a Topcon 002B HRTEM (Topcon, Tokyo, Japan) operated at 200 kV. For EDS analysis of particles collected on TEM grids, a Thermo-Noran EDS system (Waltham, MA) having a 40-mm² SiLi detector and a Noran System Six X-ray Spectral Acquisition System V2 was used to acquire EDS spectra from particles excited by a nanosized (~10 nm) electron beam probe of the TEM.

Analysis of filter material

Filter structure (pre- and posttest) and particle loading (posttest) were analyzed using SEM and EDS. Filter porosity was analyzed using a Quantachrome PoreMaster 33 mercury intrusion porosimeter. Porosity data were collected over a single intrusion/extrusion cycle. Each filter sample was analyzed with 0.5-cm³ stem volumes in glass cells. The sample masses used were about 0.02 g each for fiberglass samples and ~0.03 g for quartz samples. The contact angle and surface tension of the mercury were set to the default values of 140° on intrusion and extrusion. Low-pressure (pneumatic) data were taken from the minimum starting pressure of ~1.4 kPa (0.2 lb/in²) up to 345 kPa (50 lb/in²). All low-pressure data were corrected versus a low-pressure blank run to minimize artifacts at the low starting pressures used. High-pressure data were taken from 140 kPa (20 lb/in²) up to 230,000 kPa (33,000 lb/in²). Data sets were merged using Quantachrome Poremaster for Windows 5.10, and the intrusion cycle data were used for calculation of average (volume median) pore size and pore size distribution in filter samples. The overall range of analytical pressures employed for analyzing filters corresponded to an overall pore size range of ~1.1 mm to ~6.5 nm.

Results and Discussion

Carbon nanotubes

The synthesis products, MWCNTs formed by low-temperature synthesis, were collected on a substrate placed in the synthesis chamber tube (Figure 1); the substrate then was analyzed to assess the growth of synthesized nanotubes. These studied MWCNTs were horizontally aligned on the substrate, and were analyzed using SEM. MWCNTs were in a mixture of agglomerated and individual nanotube clusters, as seen in Figures 2a and 2b. The formed nanotube products on substrate were fibers with length of submicrometer or micrometer range and with diameter of nanometer range (Figure 2b). Nanotubes products and by-products were also found in the exhaust air during synthesis; these nanotubes were collected on the TEM grid placed in line with the exhaust tube exiting the metal flange of the glass chamber (Figure 1). The exhaust tube connecting to metal flange was measured to its exhaust air temperature of 79°F at 10 cm, 76.1°F at 15 cm, and 77.7°F at 20 cm from the metal flange. The general room temperature was 76–78°F; the filter placed at 15 cm further from the exhaust flange was collecting aerosols at room temperature. Typical collected nanotubes, as shown in the TEM images of

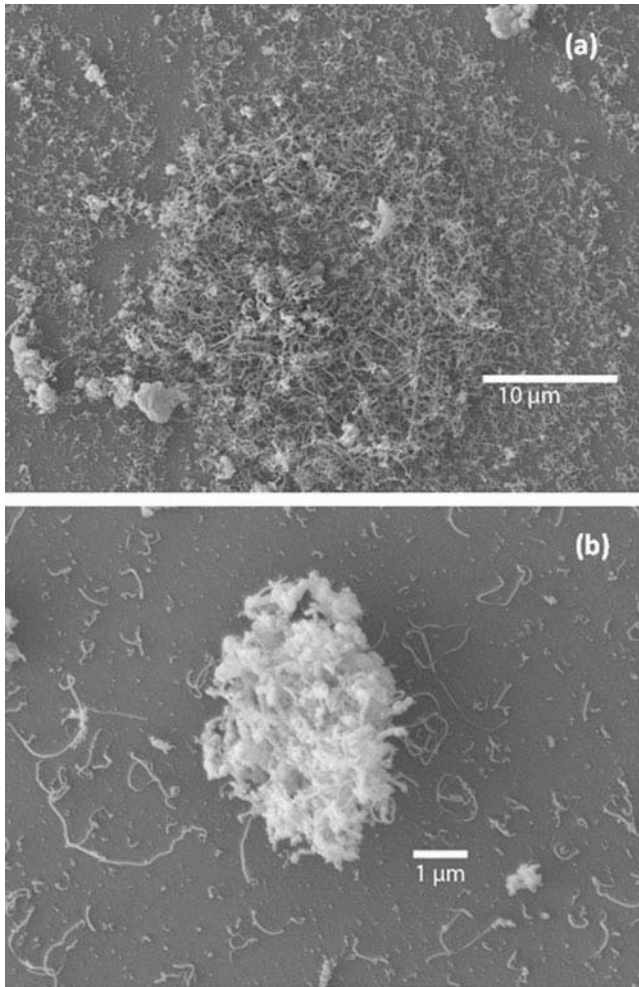


Figure 2. MWCNTs growth on substrate: (a) clusters of nanotubes, and (b) scattered individual and small agglomerate nanotubes on edge side of substrate.

Figure 3, were clusters of nanotubes with diameters ranging from 6 to 28 nm in Figure 3a and the agglomerate size of submicrometer to several micrometers; small individual nanotubes were also found, as seen in Figure 3b. Nanotubes collected on the grid during 800°C synthesis were smaller in diameter than the MWCNT product on the substrate. Particles in the exhaust gas generated during high-temperature synthesis were collected on the grid as well, and they were found to consist of spherical particles and fine fiber filaments, as seen in Figure 3c.

Collection of exhaust particles on filters

Three types of single filters, namely, SFCA, A/E, and quartz, were used to collect particles at exhaust gas during the normal (800°C) temperature operation when nanotubes and fibers primarily were emitted in the exhaust. Nanotubes seen in the exhaust (Figures 3a and 3b) were not found on the TEM grid located downstream from each test filter. However, for the higher temperature synthesis producing mostly spherical particles in the exhaust, those small agglomerates of spherical particles were found, as shown in Figure 3d, being

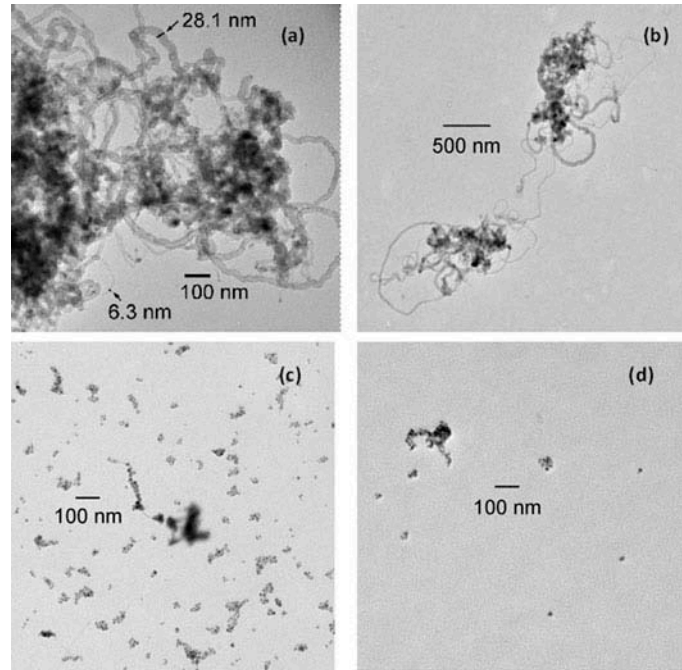


Figure 3. Particles in exhaust gas collected on TEM grid: (a) a portion of a large nanotube cluster, (b) two nanotube clusters, (c) spherical particles and fine filament, and (d) spherical particles passing SFCA filter. Panels (a) and (b) are low-temperature results, (c) and (d) are high-temperature results.

collected on the TEM grid downstream from the SFCA filter. Such particles were not found on the grid downstream from the A/E and quartz filters.

These three types of filters, quartz, A/E, and SFCA, were characterized using SEM and EDS as shown in Figures 4A, 4B, and 4C, respectively. Each type of filter was analyzed in unused and used condition. The unused filter surface exhibited clean and smooth fiber surfaces, as seen in images A1, B1, and C1 of Figure 4. Three filters after collecting exhaust particles at the normal temperature have shown yellowish tan color deposition on the contacting top surface of filter, and SEM analysis has shown bead-shaped agglomerates formed on most filter fibers, as seen in images A2, B2, and C2 of Figure 4 for three types of filter, respectively. The filter fiber surface of the used filter was carpeted by the emitted substance. These deposited and formed agglomerates in beaded shape were seen on filters used at both normal- and high-temperature synthesis. The beaded-shape agglomerate formed on the quartz filter was examined at a magnification of 20,000 as shown in Figure 4A3; fine fibers that were likely nanotubes were observed surrounding the beaded-agglomerate, and similar fibers were observed on most beaded-shape agglomerates seen in image A2 of Figure 4.

The prefilter, an SFCA filter, used at the exhaust exit collected emitted particles and was found to have dark brown and black color depositions on the collecting surface, which apparently accumulated more deposited particles than other filters. A typical SEM image of the deposited surface is shown in image C3 of Figure 4; filter fibers were thickly covered and there were three types of particle agglomerates found on filter as

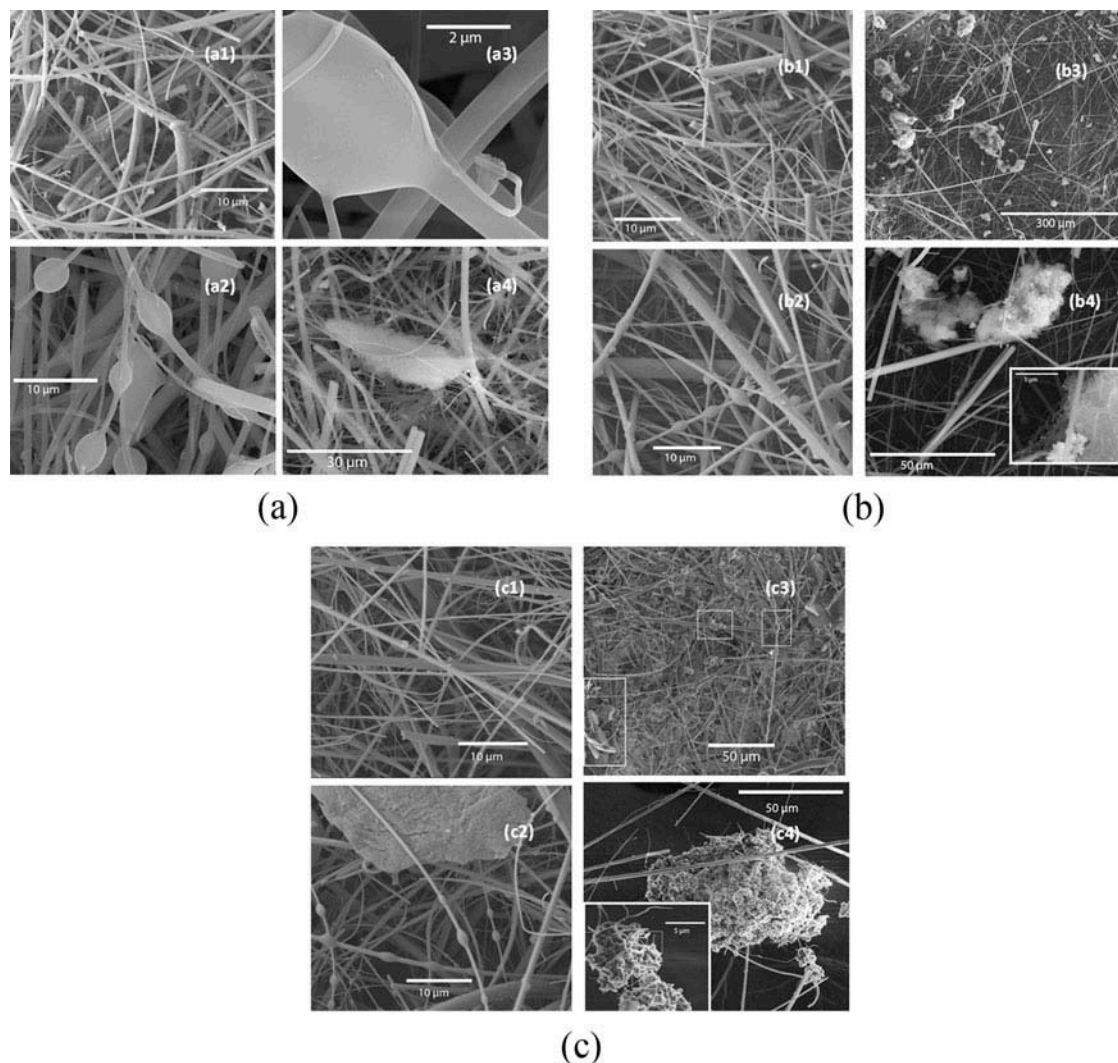


Figure 4. SEM images of clean filters and collected particle agglomerates on used filters: (a1) quartz filter before use, (a2) quartz filter after use, (a3) beaded agglomerate on quartz fiber, (a4) particles underneath surface of collecting side of used quartz filter, (b1) A/E fiberglass filter before use, (b2) beaded agglomerates on A/E used filter, (b3) trapped CNT agglomerates underneath surface of collecting side of used A/E filter, (b4) CNT agglomerate trapped underneath A/E filter, (c1) SFCA filter before use, (c2) beaded agglomerates on SFCA used fiber, (c3) three forms of particle agglomerates on used SFCA prefilter, and (c4) CNT agglomerates underneath used SFCA prefilter.

seen in the marked areas. Three types are beaded-shape agglomerates, nest-shape agglomerates, and layered sheet particles.

Particles trapped inside the filter were examined by peeling off the top collecting surface to analyze particles hidden underneath. Nest-shape CNT agglomerates were found on all three types of filters; however, distribution of such CNT agglomerate trapped varied in filters; many were found on the A/E fiberglass filter, as seen in image B3 of Figure 4. Such CNT consisted of CNT tangled fibers mixed with other substances and some circular agglomerates (Figure 4B4). Large agglomerates (~30 μm) with a similar form were found underneath the quartz filter surface, as seen in Figure 4A4. The nest-CNT agglomerates seen on the SFCA prefilter were also found underneath the surface of this prefilter; large CNT agglomerates (>50 μm)

attaching with small ones (5–10 μm), as shown in image C4 of Figure 4, consist of fibrous nanotubes.

Two non-fiber-shaped agglomerates, beaded and layer sheet, were analyzed for elemental composition using EDX, and results are shown in the Supplemental Materials. For the quartz filter, which consists of high-purity SiO_2 fibers, the elemental response showed mostly Si on filter material. Figure S1a and S1b in the Supplemental Materials show the comparison of elemental analysis on the beaded agglomerate on quartz filter; the full scan to the analyzed area and spot scan on the agglomerate shown in Figure S1a and S1b respectively, showed a much higher carbon percentage on the beaded agglomerate comparing to the background (full scan) that indicated this agglomerate consisted mostly carbon element which was released from MWCNT synthesis. This was expected, since

MWCNTs and other particles from the furnace are mostly carbon.

The beaded and layered sheet agglomerates on the SFCA prefilter were analyzed; images and elemental composition are shown in Figures S1c and S1d. SFCA filter contained impurities with various elements and carbon was still the highest composition. The layered sheet agglomerates at spot scan appeared to contain additional different elements than the beaded agglomerates did; however, the sources of such elements were not identified. In Figures S1c and S1d, filter fibers were observed with agglomerates wrapping the fiber. Some deposited micrometer-sized sheet particles were seen covering fibers (Figure S1d).

The released iron-encapsulated carbon nanoparticles seen in Figure 3c were identified to contain iron (Tsai et al., 2009), the catalyst used for synthesizing nanotubes. However, such iron-encapsulated carbon nanoparticles were not identified individually on the filter from images or elemental response. The amount of iron present could be minimal and too low to be detected by SEM EDX with large amounts of filter materials as background.

Tsai's study (Tsai et al., 2012) of quartz and A/E filters used to collect silica nanoparticles found that nanoparticles were deposited on filter fibers with their original forms as nanoparticle agglomerates. The different types of particle morphology found collected on filters represented a new finding. We found that a selective interaction between particles and fiber surface of filters caused this different agglomerate, which was associated with the surface chemical–physical properties. The origin of this surface interaction was shown to be surface tension between hydrophilic and hydrophobic substance causing the shape of wrapping deposition on filter fibers. All three filter materials contain silica (SiO_2) as the structural material, which results in hydrophilic fibers, while CNTs as well as carbon particle by-products are known to be hydrophobic in nature. The interaction mechanism between hydrophilic and hydrophobic surfaces is implicated for many biological and nonbiological phenomena (Faghihnejad and Zeng, 2013). Surface hydrophobicity is an important factor affecting interaction of nanometer-sized particles. It is hypothesized that the hydrophobic CNTs and carbon small agglomerates, when in contact with a hydrophilic filter fiber, form an arched surface due to the high surface tension and “wrap” onto the fiber surface and accumulate as spherical structures. Such surface interaction explains the formation of the observed spherically beaded shaped agglomerates collected on filter fibers. These formed agglomerates were special feature found on collecting emissions from this CNT synthesis on such hydrophilic filter fibers. The results found here, and this interpretation of the methodology for structure formation, are consistent with the results of Amade et al., who found similar structures when directly depositing untreated hydrophobic CNTs onto quartz fibers (Amade et al., 2014).

The deposited agglomerates were submicrometer to micrometer in size and thickness when wrapped or trapped on the fibers, which were much larger compared to the submicrometer- and nanometer-sized aerosol particles collected on TEM grids. This difference of particle collection was due to different

theory applied for particle collection at the grid and on the filter. Brownian motion was required to collect nanoparticles when the aerosol airstream passed the film surface of grids; however, this sampling technique didn't collect micrometer-sized particles due to the very low Brownian motion of the larger particles. Aerosol particles collected in this study were found to be a mixture of by-product aerosols in various sizes and shapes. Large agglomerates collected on sampling filters were identified containing nanotube fibers using SEM analysis.

Concentration measurement

Particle number concentrations in the exhaust gas with and without filters were measured; the concentration data for the normal temperature synthesis, which produced nanotubes in the exhaust gas, are shown in Figure 5a. Adjusted concentrations for particle size from 5 nm to 20 μm were measured by FMPS and APS. We observed a bimodal distribution of exhaust particles in the range of 20 to 560 nm from this synthesis, with a primary mode at 250 nm and second peak at 30 nm. For particles in the 100–560 nm range, the peak particle concentration decreased from almost 8,000 particles/ cm^3 to close to the detection limit of the FMPS for all three filters. The particle concentrations in the 20–80 nm range were slightly reduced when using the SFCA and A/E filters (Figure 5a), while the concentration when using the quartz filter was below or close to the baseline. The particle number concentrations above 560 nm as measured by the APS were <100 particles/ cm^3 for all measurements and sizes, with a slight peak in the 500–800 nm range, as seen in Figure 5a. The total particle number concentration for the complete 5 nm to 20 μm range was 88,500 particles/ cm^3 for no filter use, and this was reduced to 23,300, 36,000, and 700 particles/ cm^3 , respectively, for the SFCA, A/E, and quartz filters. The reductions of particle counts were consistently seen when using filters.

As the furnace operated at 925°C, many more nanometer-sized aerosol particles were formed as by-products in the exhaust gas, including carbon particles and small nanotube filaments (Tsai et al., 2009); consequently, an SFCA filter was used as a prefilter for the high-temperature tests. Adjusted concentrations measured using the FMPS and APS are shown in Figure 5b. Particles passing through the SFCA prefilter had a mode of 100 nm, and almost all of the particles passing through the second SFCA, A/E, and quartz filters were smaller than 100 nm with bimodal particle size distributions. The total number concentrations were 534,000, 59,000, 53,600, and 25,200 particles/ cm^3 respectively, when using one SFCA, two SFCA, SFCA with A/E, and SFCA with quartz. Filter collection efficiencies were not measured in this study since the aerosol production rate exhibited variations during the formation of nanotubes. Reduction of concentration was compared at the same time period of the synthesis process for various filter uses. The quartz filter appeared to have the highest concentration reduction for both synthesis conditions. The A/E filter appeared to have lower concentration reduction than the quartz filter, which contradicts our previously reported results that found the two filters to have equivalent performance. The difference likely was a result of practical effects

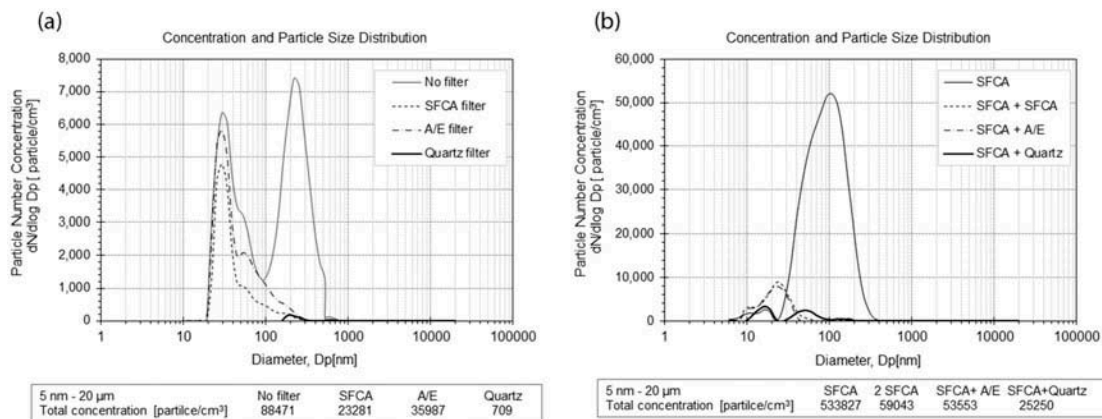


Figure 5. Particle number concentration and size distribution: (a) single filter use and (b) prefilter use.

during the synthesis operation, which had some operational variations among repeated operations that resulted in changes in the generated number concentration. A consistent result was found with similar performance of A/E and quartz filters; that is, aerosol particles were only found on the downstream TEM grid for the SFCA filter and not found for both A/E and quartz filters (Figure 3). To summarize, concentration results suggest that the A/E and quartz filters will perform effectively as CVD furnace exhaust filters based on no aerosol particles being found on grids in the exhaust passing filter, although actual collection efficiencies could not be calculated here.

Studies (Seto et al., 2010; Wang and Otani, 2012; Wang and Pui, 2013) have shown that the fibrous particles (CNTs) in a size range longer than 300 nm were collected on common sampling filters with decreased penetration comparing to spherical particles, and particles in the 100-nm range were collected with comparable efficiencies for fibrous and spherical particles. Such results were consistently seen in our study as shown in Figures 4 and 5, where particles larger than 300 nm were not seen passing through any of the filters according to the instrument readings. In addition, penetration has been found to be lower with reduced air velocity on filter; Seto et al. found that their lowest velocity of 0.05 m/s provided penetration reduction from 0.4 at 200 nm to close to 0.2 at 300 nm particle size (Seto et al., 2010). In the current study, the average air velocity (based on 2 L/min airflow) through the 47-mm filter was approximately 0.02 m/sec, which was 40% of the lowest velocity in Seto's study (Seto et al., 2010) and indicates that a penetration lower than 0.2 for particle size of 300 nm or above would be expected for the application in this process.

Filter sample porosimetry

The A/E and quartz filter samples analyzed by SEM were also analyzed via mercury intrusion porosimetry. The analysis of both A/E and quartz filters found that used filters consistently had an appreciably larger specific surface area compared to clean filters. The used quartz filter had a specific surface area approximately 20 times higher than the clean one ($\sim 0.6 \text{ m}^2/\text{g}$ for the clean quartz vs. $\sim 12.4 \text{ m}^2/\text{g}$ for the used quartz) (Table 1). The used A/E filter had a specific surface area approximately 6

Table 1. Specific surface area of analyzed A/E and quartz filters materials.

Filter type	Specific surface area (m^2/g)
Clean A/E	0.54 ^a
Used A/E	3.30 ^a
Clean quartz	0.55 ^b
Used quartz	12.35 ^b

Notes: Ratio of increases in specific surface area: quartz/(A/E) = $11.8/2.8 = \sim 4.2$.

^aA/E: $3.3 - 0.5 = 2.8 \text{ m}^2/\text{g}$ specific surface area of trapped particles.

^bQuartz: $12.4 - 0.6 = 11.8 \text{ m}^2/\text{g}$ specific surface area of trapped particles.

times higher than the clean one. The larger surface area seen on the used filters was indicative of high-surface-area particles (MWCNT, carbon fiber filaments, and particles) trapped in the filter. If we assume that the particles being trapped have the same average specific surface area in both cases, this implies that the quartz filter collected more particles than the A/E filter by about a factor of 4. This is also consistent with the greater reduction of total particle concentration during the use of the quartz filter, as discussed earlier. Quartz filters studied by Tsai et al. have shown collection efficiency above 99.5% for particles smaller than 200 nm (Tsai et al., 2012).

Conclusion

Particles in the exhaust gas released from the CVD furnace were by-products of CNT synthesis, with a primary size in nanometer range and some agglomerates in the micrometer size range. Emitted nanoparticles collected on TEM grids were in forms of nanotubes, carbon particles, and nanotube filaments. Emitted micrometer-sized particles collected on filters were found in forms of beaded-shape agglomerates wrapping around fibers, nest shape, and layered sheet agglomerates. Beaded shape and nest agglomerates containing CNT fibers were found in all three types of filters tested, where beaded agglomerates were seen mostly on the top surface. CNT fiber agglomerates were seen on the filter top surface and trapped in

the filter fibers, and had the same structure as seen collected on TEM grids. Those layered sheet particles were found to be collected on the SFCA filter when used as a prefilter at the exhaust exit of a synthesis tube, and such sheet particles were seen wrapping around filter fibers.

This practical evaluation found that the quartz filter gave a consistently higher collection ability compared to the other two tested filter types. Although the fiber diameters and porosities of the quartz and glass fiber filters were very similar, the quartz filter was about 50% thicker than the glass fiber filter, which may help explain its somewhat better performance. All filters were successful at reducing particle concentrations throughout the measured size range, and the lowest penetration size of 300 nm and above found in this study was consistent with other experimental studies (Seto et al., 2010; Wang and Otani, 2012) using fibrous particles. It has been reported that particles smaller than 100 nm would be collected more efficiently, due to their increased Brownian motion (Tsai et al., 2012) and being at lower air velocity (Seto et al., 2010). Aerosol particles released as by-products from CVD synthesis can be sufficiently collected on high-efficiency A/E and quartz filters using a well-sealed filter holder before being released into the environment.

The filters tested here were mounted in a 47-mm-diameter filter holder. However, glass and quartz fiber filter materials are also available for use in larger rectangular filter holders, such as the 20 cm × 25 cm (8 inch × 10 inch) filters used in high-volume air samplers. The use of such a larger filter would increase loading capability of the filter and would reduce the filtration velocity by a factor of thirty, thus increasing filter lifetime and enhancing nanoparticle collection by Brownian motion. A viable alternative, of course, would be to use higher efficiency HEPA filters on the furnace exhaust. The filters tested here were evaluated because of the possibility that laboratories will utilize these readily available filters rather than HEPA filters, which must be purchased in a housing that can be integrated into a furnace's exhaust system. In any case, it is vitally important, given the likely carcinogenicity of at least some CNTs, that the exhaust from CNT furnaces be filtered to prevent their release into the general environment.

Acknowledgments

The authors thank Daniel Schmidt for assistance with the filter porosity test, and Earl Ada, Rosa Diaz, and Aparna Shinde for technical support for SEM, TEM, and EDX analysis. The authors declare no conflict of interest relating to the material presented in this paper. Its contents, including any opinions and/or conclusions expressed, are those of the authors.

Funding

The research was partially supported by Nanoscale Science and Engineering Centers for High-rate Nanomanufacturing funded by the National Science Foundation (award NSF-0425826).

Supplemental Materials

Supplemental data for this paper can be accessed at the [publisher's website](#)

References

- Amade, R., S. Hussain, I.R. Ocaña, and E. Bertran. 2014. Growth and functionalization of carbon nanotubes on quartz filter for environmental applications. *J. Environ. Eng. Ecol. Sci.* 3(2). doi:10.7243/2050-1323-3-2
- Faghijnejad, A., and H. Zeng. 2013. Interaction mechanism between hydrophobic and hydrophilic surfaces: Using polystyrene and mica as a model system. *Langmuir* 29(40):12443–51, doi:10.1021/la402244h
- Golanski, L., A. Guiot, F. Rouillon, J. Pocachard, and F. Tardif. 2009. Experimental evaluation of personal protective devices against graphite nanoaerosols: Fibrous filter media, masks, protective clothing, and gloves. *Hum. Exp. Toxicol.* 28:353–59. doi:10.1177/0960327109105157
- Golanski, L., A. Guiot, and F. Tardif. 2010. Experimental evaluation of individual protection devices against different types of nanoaerosols: Graphite, TiO₂, and pt. *J. Nanopart. Res.* 12:83–89. doi:10.1007/s11051-009-9804-x
- Golanski, L., A. Guiot, and F. Tardif. 2008. Efficiency of fibrous filters and personal protective equipments against nanoaerosols. Nanosafe Dissemination Report, DR-325/326-200801-1, Project ID-NMP2-CT-2005-515843. Nanosafe2 project website: <http://www.nanosafe.org>.
- Grosse, Y., D. Loomis, K. Z. Guyton, B. Laugy-Secretan, F. El Ghissassi, V. Bouvard, L. Bernabrahim-Tallea, et al. 2014. Carcinogenicity of fluoro-edenite, silicon carbide fibres and whiskers, and carbon nanotubes. *Lancet Oncol.* 15(13):1427–28. doi:10.1016/S1470-2045(14)71109-X
- Ji, J.H., J.B. Kim, G. Lee, J.H. Noh, S.J. Yook, S.H. Cho, and G.N. Bae. 2015. Workplace exposure to titanium dioxide nanopowder released from a bag filter system. *Biomed. Res. Int.* article ID 524283. doi:10.1155/2015/524283
- Lundgren, D., and T. Gunderson. 1975. Efficiency and loading characteristics of EPA's high-temperature quartz fiber filter media. *Am. Ind. Hyg. Assoc. J.* 36:866–72. doi:10.1080/0002889758507358
- Lundgren, D., and T. Gunderson. 1976. Filtration characteristics of class fiber filter media at elevated temperatures, Environmental Sciences Research Laboratory. U.S. Environmental Protection Agency, Environmental Protection Technology Series EPA-600/2-76-192. <http://nepis.epa.gov/Adobe/PDF/91015XO6.pdf>.
- Ma-Hock, L., S. Treumann, V. Strauss, S. Brill, F. Luizi, M. Mertler, K. Wiench, A.O. Gamer, B. van Ravenzwaay, and R. Landsiedel. 2009. Inhalation toxicity of multiwall carbon nanotubes exposed in rats for 3 months. *Toxicol. Sci.* 112(2):468–81. doi:10.1093/toxsci/kfp146
- Maynard, A.D., and E.D. Kuempel. 2005. Airborne nanostructured particles and occupational health. *J. Nanopart. Res.* 7(6):587–614. doi:10.1007/s11051-005-6770-9
- Occupational Safety and Health Administration. 2006. Table Z-1 Limits for Air Contaminants. 29 CFR 1910.1000 Table Z-1. https://www.osha.gov/pls/oshaweb/owadisp.show_document?p_table=STANDARDS&p_id=9992
- Pall Corporation. 2011. Glass fiber filters, Pall product brochure. http://labfilters.pall.com/catalog/laboratory_20027.asp (accessed February 2015).
- Poland, C.A., R. Duffin, I. Kinloch, A. Maynard, W.A.H. Wallace, A. Seaton, V. Stone, S. Brown, W. MacNee, and K. Donaldson. 2008. Carbon nanotubes introduced into the abdominal cavity of mice show asbestos-like pathogenicity in a pilot study. *Nat. Nanotech.* 3:423–28. doi:10.1038/nnano.2008.111
- Rengasamy, S., B.C. Eimer, and R.E. Shaffer. 2009. Comparison of nanoparticle filtration performance of NIOSH-approved and CE-marked particulate filtering facepiece respirators. *Ann. Occup. Hyg.* 53(2):117–28. doi:10.1093/annhyg/men086
- Rengasamy, S., W.P. King, B.C. Eimer, and R.E. Shaffer. 2008. Filtration performance of NIOSH-approved N95 and P100 filtering facepiece respirators against 4 to 30 nanometer-size nanoparticles. *J. Occup. Environ. Hyg.* 5(9):556–64. doi:10.1080/15459620802275387
- Ryman-Rasmussen, J.P., M.F. Cesta, A.R. Brody, J.K. Shipley-Phillips, J.I. Everitt, E.W. Tewksbury, O.R. Moss, et al. 2009. Inhaled carbon nanotubes

- reach the subpleural tissue in mice. *Nat. Nanotech.* 4:747–51. doi:10.1038/nnano.2009.305
- Seto, T., T. Furukawa, Y. Otani, K. Uchida, and S. Endo. 2010. Filtration of multi-walled carbon nanotube aerosol by fibrous filters. *Aerosol Sci. Technol.* 44:734–40. doi:10.1080/02786826.2010.487881
- Shvedova, A.A., E.R. Kisin, R. Mercer, A.R. Murray, V.J. Johnson, A.I. Potapovich, Y.Y. Tyurina, et al. 2005. Unusual inflammatory and fibrogenic pulmonary responses to single-walled carbon nanotubes in mice. *Am. J. Physiol. Lung Cell. Mol. Physiol.* 289:698–708. doi:10.1152/ajplung.00084.2005
- Shvedova, A.A., E.R. Kisin, A.R. Murray, V.J. Johnson, O. Gorelik, S. Arepalli, A.F. Hubbs, et al. 2008. Inhalation vs. aspiration of single-walled carbon nanotubes in C57BL/6 mice: Inflammation, fibrosis, oxidative stress, and mutagenesis. *Am. J. Physiol. Lung Cell. Mol. Physiol.* 295:L552–65. doi:10.1152/ajplung.90287.2008
- Smith, B.D., and S.B.H. Bach. 2015. Deposition of carbon nanotubes in commonly used sample filter media. *Global J. Environ. Sci. Manage.* 1(3):189–98.
- Takagi, A., A. Hirose, T. Nishimura, N. Fukumori, A. Ogata, N. Ohashi, S. Kitajima, and J. Kanno. 2008. Induction of mesothelioma in p53^{+/-} mouse by intraperitoneal application of multi-wall carbon nanotube. *J. Toxicol. Sci.* 33(1):105–16. http://www.jstage.jst.go.jp/article/jts/33/1/33_105/_article. doi:10.2131/jts.33.105
- Tsai, C.S.J. 2015. Characterization of airborne nanoparticle loss in sampling tubing. *J. Occup. Environ. Hyg.* doi:10.1080/15459624.2015.1019077
- Tsai, S.J., M. Echevarría-Vega, G. Sotiriou, C. Santeufemio, C. Huang, D. Schmidt, P. Demokritou, and M. Ellenbecker. 2012. Evaluation of environmental filtration control of engineered nanoparticles using the harvard versatile engineered nanomaterial generation system (VENGES). *J. Nanopart. Res.* 14:812. doi:10.1007/s11051-012-0812-x
- Tsai, S.J., M. Hofmann, M. Hallock, E. Ada, J. Kong, and M.J. Ellenbecker. 2009. Characterization and evaluation of nanoparticle release during the synthesis of single-walled and multi-walled carbon nanotubes by chemical vapor deposition. *Environ. Sci. Technol.* 43(15):6017–23. doi:10.1021/es900486y
- Wang, C., and Y. Otani. 2012. Removal of nanoparticles from gas streams by fibrous filters: A review. *Ind. Eng. Chem. Res.* doi:10.1021/ie300574m.
- Wang, J., and D. Pui. 2013. Dispersion and filtration of carbon nanotubes (CNTs) and measurement of nanoparticle agglomerates in diesel exhaust. *Chem. Eng. Sci.* 85:69–76. doi:10.1016/j.ces.2011.12.045
- Whatman GE Healthcare. 2011. Whatman filter, air sampling filters and quartz filters. <http://www.whatman.com/AirSamplingandQuartzFilters.aspx> (accessed February 2015).
- Xiang, R., G. Luo, W. Qian, Y. Wang, F. Wei, and Q. Li. 2007. Large area growth of aligned CNT arrays on spheres: Towards the large scale and continuous production. *Chem. Vap. Dep.* 13(10):533–36. doi:10.1002/cvde.200704249

About the Authors

Candace Su-Jung Tsai works in the Department of Environmental and Radiological Health Science at the College of Veterinary Medicine and Biomedical Science.

Mario Hofmann works in the Department of Materials Science and Engineering at the National Cheng Kung University.

Marilyn Hallock works in the Department of Environment, Health and Safety at the Massachusetts Lowell.

Michael Ellenbecker works in the Toxics Use Reduction Institute at the University of Massachusetts Lowell.

Jing Kong works in the Department of Electrical Engineering and Computer Science at the Massachusetts Institute of Technology.